

Outlier-Robust Neural Network Training: Efficient Optimization of Transformed Trimmed Loss with Variation Regularization

Akifumi Okuno^{*1,2} and Shotaro Yagishita¹

¹The Institute of Statistical Mathematics

²RIKEN Center for Advanced Intelligence Project

Abstract

In this study, we consider outlier-robust predictive modeling using highly-expressive neural networks. To this end, we employ (1) a transformed trimmed loss (TTL), which is a computationally feasible variant of the classical trimmed loss, and (2) a higher-order variation regularization (HOVR) of the prediction model. Note that using only TTL to train the neural network may possess outlier vulnerability, as its high expressive power causes it to overfit even the outliers perfectly. However, simultaneously introducing HOVR constrains the effective degrees of freedom, thereby avoiding fitting outliers. We newly provide an efficient stochastic algorithm for optimization and its theoretical convergence guarantee. (*Two authors contributed equally to this work.)

1 Introduction

Highly non-linear parametric models, such as deep neural networks, have gained significant attention due to their impressive expressive power (Goodfellow et al., 2016; Sze et al., 2017; Miikkulainen et al., 2019; Samek et al., 2021). These models can approximate arbitrary continuous functions (Cybenko, 1989; Yarotsky, 2017), making them highly adaptive to complex target functions. This expressive power enables the capture of complex patterns, as demonstrated in large language models (Brown et al., 2020; Liu et al., 2023) for modeling human language structures. However, this flexibility also presents the risk of overfitting, where the model can fit not only the true underlying patterns but also noise in the training data, particularly when the data size is limited.

In the presence of outliers, overfitting becomes an even more serious issue. Outliers can cause models to learn patterns that are not representative of the general data distribution. A straightforward approach to mitigate this problem is to use robust loss functions, such as the trimmed loss (Rousseeuw, 1984), which reduces the influence of outliers by discarding the several largest sample-wise losses. However, simply applying robust loss, including trimmed loss, is not enough to fully solve the issue, especially with highly expressive models like neural networks. Unlike linear models whose limited expressive power helps robust loss functions ignore outliers, these highly expressive models may still overfit to the remaining outliers, thus negating the intended outlier-resilience of the robust loss functions.

*okuno@ism.ac.jp

To fully exploit the trimmed loss robustness, we introduce higher-order variation regularization (HOVR), which builds on the concept of total variation (Rudin et al., 1992; Koenker and Mizera, 2004; Bredies and Holler, 2020). HOVR helps control the model’s expressiveness by constraining the degrees of freedom, preventing the network from overfitting to outliers while maintaining its flexibility to capture complex patterns. By combining trimmed loss with HOVR, we can leverage the full advantages of robust loss functions and ensure that the neural network is estimated in a manner that is both flexible and resilient to outliers.

However, optimizing trimmed loss and HOVR poses computational challenges. Trimmed loss requires sorting sample-wise losses, and HOVR involves integrating the variations of the neural network, making direct optimization difficult. To address this, we propose an augmented and regularized trimmed loss (ARTL), that combines a transformed trimmed loss (TTL), a more computationally efficient form of trimmed loss developed by Yagishita (2024), and HOVR. We introduce a stochastic gradient-supergradient descent (SGSD) algorithm to minimize ARTL. In line with Robbins and Monro (1951), Ghadimi and Lan (2013), and Bottou et al. (2018), we prove its theoretical convergence, resulting in robust and efficient training of neural networks. See Figure 1 for an illustration of our approach.

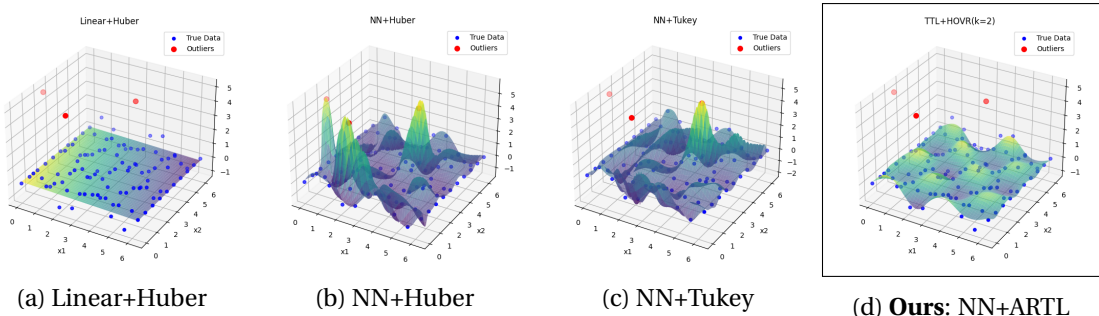


Figure 1: Illustration of our proposed approach, using the wave-like function $f_*(x) = \sin(2x_1) \cos(2x_2)$. This function is later referred to as the ‘checkered’ function due to the checkered appearance of its contour plot. (a): The linear model cannot capture complex patterns. (b) and (c): Neural networks (NNs) without variation regularization may overfit to outliers, even when using robust loss functions such as Huber’s or Tukey’s, due to the excessive degrees of freedom in the network. (d): Our proposed approach effectively ignores the outliers while preserving the expressive power. See Section 4.1 for more details of the synthetic dataset experiments. Note that the simple weight decay, often used to treat singularity in the loss, usually does not address this issue.

1.1 Related Works

This section discusses related works on the key concepts of this paper: HOVR and TTL.

Works Related to HOVR

Various heuristic approaches have been proposed to prevent overfitting in neural network training, such as dropout (Srivastava et al., 2014), early stopping (e.g., Yao et al. (2007)), data augmentation (e.g., Hernández-García and König (2018); Zhang et al. (2021)), and batch normalization (Luo et al., 2019). These methods are considered forms of regularization and can be combined with parameter regularization, also called weight decay (Kingma and Ba, 2014; Goodfellow et al., 2016).

Total variation (TV) regularization (Rudin et al., 1992; Engl et al., 1996; Osher et al., 2005) has been applied to regression models using splines (Stone, 1994; Mammen and van de Geer, 1997), kernels (Zou and Hastie, 2005), and triograms (Koenker and Mizera, 2004). TV has been extended to second order (Koenker and Mizera, 2004; Hinterberger and Scherzer, 2006; Duan et al., 2015) and general order ($k \in \mathbb{N}$) (Bredies and Holler, 2020), with optimization via discrete approximations. In neural networks, neural splines (Williams et al., 2021) approximate second-order TV terms through finite approximations. The representer theorem is also studied in Banach space (Parhi and Nowak, 2021) with TV terms measured in the Radon domain. These theories have been further developed (Parhi and Nowak, 2022; Unser, 2023; Bartolucci et al., 2023), but practical optimization algorithms remain underdeveloped.

Works Related to TTL

Robust loss functions have largely been developed following the seminal work of Beaton and Tukey (1974), Huber and Ronchetti (1981) and Rousseeuw (1984). Building on this foundation, Yagishita (2024) introduces an innovative approach that transforms sparse least trimmed squares (SLTS) into a more tractable problem, making it solvable via a deterministic proximal gradient method. This method exhibits strong convergence properties for linear models, outperforming FAST-LTS (Alfons et al., 2013) and TSVRG (Aravkin and Davis, 2020) in speed and offering potentially strong convergence. While these studies are grounded in proximal methods, our study adopts a stochastic approach, while preserving the idea of transforming trimmed loss into a more manageable form.

While convergence for nonlinear models has been addressed, proximal methods can be less efficient, particularly in our case where computing the full gradient of the integral-based HOVR term is intractable. To overcome this, we propose a stochastic approach. The convergence of stochastic proximal gradient-type methods for non-smooth, non-convex problems has been explored by Xu et al. (2019b); Metel and Takeda (2019); Xu et al. (2019a); Metel and Takeda (2021); Yun et al. (2021); Deleu and Bengio (2021). However, Xu et al. (2019b) and Metel and Takeda (2019, 2021) assume Lipschitz continuity for the non-convex regularization term, which is not applicable in our context. Additionally, Xu et al. (2019a), Yun et al. (2021), and Deleu and Bengio (2021) require increasing mini-batch size for convergence, which is impractical for real-world use. Note that TSVRG (Aravkin and Davis, 2020) is not suited to our problem setting.

2 Outlier-Robust Neural Network Training

We describe a multi-layer perceptron, referred to here as a neural network, in Section 2.1. The key concepts of TTL and HOVR, which are used to define the proposed ARTL, are introduced in Sections 2.2 and 2.3, respectively. Following this, we propose SGSD algorithm in Section 2.4, and it leverages a specifically-designed practical stochastic gradient defined in Section 2.5. To enhance clarity, Section 2.6 examines a simplified case of HOVR using more basic linear basis function models.

2.1 Neural Network

Let $J, n \in \mathbb{N}$ be the dimension of the covariate and the sample size, respectively. For each $j = 1, 2, \dots, J$, let $D_j^-, D_j^+ \in \mathbb{N}$ define the support of the covariate, with $D_j^- < D_j^+$; we then define the compact covariate space as $\Omega := \prod_{j=1}^J [D_j^-, D_j^+]$. We denote the observations as pairs $(x_i, y_i) \in \Omega \times \mathbb{R}$, for $i = 1, 2, \dots, n$.

We consider training the regression model $f_\theta : \Omega \rightarrow \mathbb{R}$ parameterized by $\theta \in \Theta \subset \mathbb{R}^r$ ($r \in \mathbb{N}$), such that $f_\theta(x_i)$ closely approximates $f_*(x_i) = \mathbb{E}[y_i|x_i]$. For simplicity, this study employs a multi-layer perceptron

$$\text{(MLP): } f_\theta(x) = (l_\theta^{(Q)} \cdot \tilde{l}_\theta^{(Q-1)} \dots \tilde{l}_\theta^{(0)})(x),$$

where $l_\theta^{(q)}(x) = A^{(q)}x + b^{(q)}$ denotes a linear function, and $\sigma : \mathbb{R} \rightarrow \mathbb{R}$ represents an activation function (with $\sigma(z)$ applied element-wise if z is a vector). Here, $\tilde{l}_\theta^{(q)} = \sigma \circ l_\theta^{(q)}$. Typical choice for σ includes the sigmoid function $\sigma(z) = 1/\{1 + \exp(-z)\}$ or the hyperbolic tangent function $\sigma(z) = \{\exp(z) - \exp(-z)\} / \{\exp(z) + \exp(-z)\}$. MLP is known as a specific architecture of the neural network having the universal approximation capability (Cybenko, 1989; Yarotsky, 2017), and MLP with large $Q \gg 0$ is also known as a deep neural network (Goodfellow et al., 2016).

The parameters to be estimated in this MLP are $\theta = (\{A^{(q)}, b^{(q)}\}_{q=0}^Q)$, where $A^{(q)} \in \mathbb{R}^{L_{q+1} \times L_q}$ and $b^{(q)} \in \mathbb{R}^{L_{q+1}}$ are defined with the user-specified number of hidden units $L_1, L_2, \dots, L_Q \in \mathbb{N}$. The input and output dimensions are specified as $L_0 = J$ and $L_{Q+1} = 1$.

While we focus on the MLP in this study, it is worth noting that the following discussion can be extended to arbitrary regression models, including splines and kernel regression models.

2.2 TTL

To train the neural network, this section defines TTL. Let the residual be $r_i(\theta) = y_i - f_\theta(x_i)$ and denote the sorted indices by $(1; \theta), (2; \theta), \dots, (n; \theta)$, where they satisfy $|r_{(1; \theta)}(\theta)| \leq |r_{(2; \theta)}(\theta)| \leq \dots \leq |r_{(n; \theta)}(\theta)|$. Given a user-specified hyperparameter $h \in \mathbb{N}$ and the residual vector $r(\theta) = (r_1(\theta), r_2(\theta), \dots, r_n(\theta))$, the h -trimmed loss (Rousseeuw, 1984) is defined as:

$$T_h(r(\theta)) = \frac{1}{n} \sum_{i=1}^h r_{(i; \theta)}^2(\theta),$$

which aims to mitigate the adverse effect of outliers by discarding the $(n - h)$ -largest sample-wise losses. In our implementation, for instance, we employ $h = 0.9n$. Yagishita (2024) demonstrates that for arbitrary function f_θ , including neural networks, minimizing $T_h(r(\theta))$ is equivalent to minimizing the TTL:

$$\min_{\xi \in \mathbb{R}^n} \left\{ \frac{1}{n} \|r(\theta) - \xi\|_2^2 + T_h(\xi) \right\} = \frac{1}{2} T_h(r(\theta)), \quad (1)$$

which is more computationally tractable, as discussed in Section 2.4. While TTL helps discard the influence of outliers, highly expressive models like neural networks may still overfit to outliers, even with robust loss functions. See, e.g., Figure 1 for the outlier-vulnerability of the traditional Huber's and Tukey's robust loss functions used to train neural networks. To address this, we introduce an effective regularization called HOVR in Section 2.3.

2.3 HOVR

To introduce HOVR, we first revisit the regularization of linear basis function models, $f_\theta^\dagger(x) = \sum_{l=1}^L \theta_l \phi_l(x)$, which encompasses linear, kernel, and spline regression models. In this context, the parameter regularization $\|\theta\|_2^2$ corresponds to the function norm of f_θ^\dagger , specifically $\|f_\theta^\dagger\|_{L^2(\Omega)}^2 = \int_\Omega f_\theta^\dagger(x)^2 dx$, as discussed in Supplement A. However, this interpretation is limited to linear models

and does not extend to more expressive neural networks. Therefore, for more expressive models, it is more natural to design the regularization term directly. We thus define the HOVR term:

$$C_{k,q}(f_\theta) = \sum_{\mathbf{i}} w_{\mathbf{i}} \int_{\Omega} \left| \nabla_{\mathbf{i}}^{[k]} f_\theta(x) \right|^q dx, \quad (2)$$

instead of the simple parameter regularization. Here, $k \in \{0, 1, 2, \dots\}$ and $q > 0$ are user-specified parameters, and $w_{\mathbf{i}} \geq 0$ denotes the weight satisfying $\sum_{\mathbf{i}} w_{\mathbf{i}} = 1$, and $\nabla_{\mathbf{i}}^{[k]} = \partial^k / \partial x_{i_1} \partial x_{i_2} \cdots \partial x_{i_k}$ denotes the differentiation with $\mathbf{i} = (i_1, i_2, \dots, i_k)$, indicating that $C_{k,q}(f)$ regularizes the q th powered variation of the k th derivative of f_θ . This derivative $\nabla_{\mathbf{i}}^{[k]} f_\theta(x)$ can be easily computed, for instance, by Autograd in PyTorch (<https://pytorch.org/>).

While there is no practical regularization exactly identical to (2) to the best of authors' knowledge, it encompasses various forms of regularization: (1, 1)-VR is also known as a total variation (Rudin et al., 1992; Engl et al., 1996; Osher et al., 2005), and it is further generalized to the 2nd order ($k = 2$; Koenker and Mizera, 2004; Hinterberger and Scherzer, 2006) and general order ($k \in \mathbb{N}$; Bredies and Holler, 2020).

It is worth noting that the integral term in HOVR (2) is generally difficult to expand explicitly. However, this integral-based term can be efficiently optimized in a stochastic manner, as demonstrated in Section 2.4.

2.4 Proposal: ARTL and SGSD

Simply combining trimmed loss and HOVR, we define the regularized trimmed loss:

$$\frac{1}{2} T_h(r(\theta)) + \lambda C_{k,q}(f_\theta). \quad (3)$$

Considering the equivalent expression of TTL (1), minimizing this regularized trimmed loss (3) is equivalent to minimizing the augmented and regularized trimmed loss (ARTL)

$$F_{h,\lambda}(\theta, \xi) = U_\lambda(\theta, \xi) - V_h(\xi)$$

with respect to the augmented parameter (θ, ξ) , where

$$\begin{aligned} U_\lambda(\theta, \xi) &= \frac{1}{n} \{ \|r(\theta) - \xi\|_2^2 + \|\xi\|_2^2 \} + \lambda C_{k,q}(f_\theta), \\ V_h(\xi) &= \frac{1}{n} \|\xi\|_2^2 - T_h(\xi), \end{aligned}$$

are nonconvex smooth, and convex non-smooth functions, respectively. As the former $U_\lambda(\theta, \xi)$ is smooth, we can define its stochastic gradient $u_\lambda^{(t)}(\theta, \xi)$ that unbiasedly estimates the gradient $\partial U_\lambda(\theta, \xi) / \partial(\theta, \xi)$; see Section 2.5 for our implementation. For the latter nondifferentiable function $V_h(\xi)$, we define its subgradient $(0, \nu_h(\xi))$, where $\nu_h(\xi)$ is a member of the subdifferential set $\{\nu \mid \forall \xi', V_h(\xi') \geq V_h(\xi) + \langle \nu, \xi' - \xi \rangle\}$. Namely, $-(0, \nu_h(\xi))$ is the supergradient of $-V_h$. Then, we define the stochastic gradient-supergradient:

$$g_{h,\lambda}^{(t)}(\theta, \xi) = u_\lambda^{(t)}(\theta, \xi) - (0, \nu_h(\xi)).$$

With inspiration from the difference-of-convex algorithm, we propose a stochastic gradient-supergradient descent (SGSD) algorithm that updates the parameters $(\theta^{(t)}, \xi^{(t)})$ at iteration t by:

$$(\theta^{(t+1)}, \xi^{(t+1)}) \leftarrow (\theta^{(t)}, \xi^{(t)}) - \omega_t g_{h,\lambda}^{(t)}(\theta^{(t)}, \xi^{(t)}).$$

Since the proximal mapping of T_h can be computed efficiently (Yagishita, 2024), one may consider applying stochastic proximal gradient methods. However, proximal methods require the mini-batch size to be increased indefinitely to ensure convergence when dealing with integral-based regularization terms. This makes them unsuitable for our specific problem. In contrast, SGSD does not have this requirement as presented in Section 3.

SGSD in Practical Scenarios: The stochastic gradient-supergradient $g_{h,\lambda}^{(t)}(\theta, \xi)$ reduces to the standard stochastic gradient of $F_{h,\lambda}(\theta, \xi)$ at differentiable points. Since differentiable points are present almost everywhere in the parameter space, the proposed SGSD, whose convergence is rigorously proven in Section 3, is essentially equivalent to standard SGD when applied to ARTL in practical scenarios. Therefore, our analysis also can be regarded as a strong theoretical evidence for the SGD applied to robust regression using neural networks.

2.5 A Practical Stochastic Gradient

To complete the definition of SGSD presented in Section 2.4, this section provides a practical construction of the stochastic gradient $u_\lambda^{(t)}(\theta^{(t)}, \xi^{(t)})$, which serves as an unbiased estimate of the smooth function $U_\lambda(\theta, \xi)$. The stochastic gradient is employed instead of the deterministic gradient because the gradient of $U_\lambda(\theta, \xi)$ includes an integral term arising from the HOVR term (2).

We begin by specifying the hyperparameter $M^{(t)} \in \mathbb{N}$, and subsequently generate i.i.d. random numbers $\mathcal{Z}^{(t)} := \{z_1^{(t)}, z_2^{(t)}, \dots, z_{M^{(t)}}^{(t)}\}$ from a uniform distribution over the set Ω . We then define:

$$u_\lambda^{(t)}(\theta^{(t)}, \xi^{(t)}) = \frac{1}{n} \frac{\partial \{\|r(\theta^{(t)}) - \xi^{(t)}\|_2^2 + \|\xi^{(t)}\|_2^2\}}{\partial(\theta, \xi)} + \lambda \sum_{\mathbf{i}} w_{\mathbf{i}} \frac{1}{M} \sum_{z \in \mathcal{Z}^{(t)}} \frac{\partial |\nabla_{\mathbf{i}}^{[k]} f_\theta(z)|^q}{\partial(\theta, \xi)}, \quad (4)$$

and it unbiasedly estimates the gradient of U_λ as:

$$\mathbb{E}[u_\lambda^{(t)}(\theta^{(t)}, \xi^{(t)})] = \frac{\partial U_\lambda(\theta^{(t)}, \xi^{(t)})}{\partial(\theta, \xi)}$$

under the assumption that the order of operations can be exchanged. Given the general difficulty of deriving an explicit form of HOVR and the computational infeasibility of performing numerical integration at each step of gradient descent, this stochastic gradient is defined to bypass the need for integration.

2.6 Simpler Case: Basis Function Models

For simplicity, we consider the case of univariate input: $J = 1$. Using the linear basis function models $f_\theta^\dagger(x) = \sum_{l=1}^L \theta_l \phi_l(x)$, we obtain the identity:

$$C_{k,2}(f_\theta^\dagger) = \|\nabla^{[k]} f_\theta^\dagger\|_{L^2(\Omega)}^2 = \langle \theta, G^{[k]} \theta \rangle,$$

where the matrix $G^{[k]} = \int_{\Omega} (\nabla^{[k]} f_\theta^\dagger(x))^{\otimes 2} dx$ defined with $A^{\otimes 2} = AA^\top$ is non-negative definite. See Supplement A for the derivation. Therefore, our approach, applied to basis function models, corresponds to trimmed-loss regression using ridge-type parameter regularization. This study provides its extension: we consider the regularization term $C_{k,q}(f_\theta^\dagger)$ not only for basis function models but also more complex models including neural networks.

3 Convergence Analysis

In this section, we present the convergence properties of SGSD. All proofs are provided in Supplement B.

The following assumptions form the basis of our analysis: let \mathcal{F}_t denote the natural filtration associated with $(\theta^{(t)}, \xi^{(t)})$, and let \mathbb{E}_t represent the conditional expectation, $\mathbb{E}[\cdot | \mathcal{F}_t]$.

Assumption 1. We assume the following conditions:

- (a) $\partial U_\lambda / \partial(\theta, \xi)$ is Lipschitz continuous with a Lipschitz constant $L > 0$;
- (b) $\mathbb{E}_t[u_\lambda^{(t)}(\theta^{(t)}, \xi^{(t)})] = \partial U_\lambda(\theta^{(t)}, \xi^{(t)}) / \partial(\theta, \xi)$;
- (c) There exist $\mu_1, \mu_2 > 0$ such that

$$\mathbb{E}_t[\|g_{h,\lambda}^{(t)}(\theta^{(t)}, \xi^{(t)})\|_2^2] \leq \mu_1 + \mu_2 \mathbb{E}_t[\|g_{h,\lambda}(\theta^{(t)}, \xi^{(t)})\|_2^2],$$

where $g_{h,\lambda}(\theta^{(t)}, \xi^{(t)}) = \mathbb{E}_t[g_{h,\lambda}^{(t)}(\theta^{(t)}, \xi^{(t)})]$.

Assumption 1(a) is used commonly for first-order methods in optimization (Bottou et al., 2018). Assumption 1(b) asserts the unbiasedness of the stochastic gradient. By defining $\Delta u_\lambda^{(t)} := u_\lambda^{(t)}(\theta^{(t)}, \xi^{(t)}) - \partial U_\lambda(\theta^{(t)}, \xi^{(t)}) / \partial(\theta, \xi)$, the boundedness condition $\mathbb{E}_t[\|\Delta u_\lambda^{(t)}\|_2^2] \leq \sigma^2$, which is commonly used in the analysis of stochastic gradient descent, implies Assumption 1(c), which is a natural extension of Assumption 4.3 in Bottou et al. (2018). For a detailed derivation, refer to Supplement B.1.

Due to the strictness of the notation, we herein consider the convergence of a criticality measure

$$\begin{aligned} C(\theta, \xi) &:= \text{dist}(\partial U_\lambda(\theta, \xi) / \partial(\theta, \xi), \{0\} \times \partial V_h(\xi)) \\ &= \inf_{v \in \partial V_h(\xi)} \|\partial U_\lambda(\theta, \xi) / \partial(\theta, \xi) - (0, v)\|_2. \end{aligned}$$

With the unbiasedness assumption, roughly speaking, the convergence of the critical measure leads to the convergence of $g_{h,\lambda}(\theta^{(t)}, \xi^{(t)})$ up to the subdifferential difference. It also indicates the gradient-supergradient of ARTL converges to 0. See Theorem 1 for the convergence of the criticality measure.

Theorem 1. Let T be a natural number representing the number of SGSD iterations. Suppose that Assumption 1 holds and that the learning rate satisfies $0 < \omega_s < 2 / (L\mu_2)$ for $s = 0, 1, \dots, T$. Then, we have

$$\mathbb{E}[C(\theta^{(\tau_T)}, \xi^{(\tau_T)})] \leq \left\{ \frac{2F_{h,\lambda}(\theta^{(0)}, \xi^{(0)}) + L\mu_1 \sum_{t=0}^T \omega_t^2}{\sum_{t=0}^T (2\omega_t - L\mu_2 \omega_t^2)} \right\}^{1/2},$$

where the stopping time $\tau_T \in \{0, 1, \dots, T\}$ is randomly chosen independently of $\{(\theta^{(t)}, \xi^{(t)})\}$, with the probability for $s = 0, 1, \dots, T$:

$$\mathbb{P}(\tau_T = s) = \frac{2\omega_s - L\mu_2 \omega_s^2}{\sum_{t=0}^T (2\omega_t - L\mu_2 \omega_t^2)}.$$

Considering the rate of convergence, we last discuss the learning rate schedule. If we use common diminishing learning rates that satisfy

$$\sum_{t=0}^{\infty} \omega_t = \infty, \text{ and } \sum_{t=0}^{\infty} \omega_t^2 < \infty, \quad (5)$$

the expected measure $\mathbb{E}[C(\theta^{(\tau_T)}, \xi^{(\tau_T)})]$ converges to 0 as $T \rightarrow \infty$. A typical choice, such as $\omega_t = \alpha t^{-1}$, yields a convergence rate of $\mathcal{O}((\log T)^{-1/2})$. However, there exist alternative learning rate schedules that achieve faster convergence, even though they violate the condition (5). See Corollary 1.

Corollary 1. Suppose that Assumption 1 holds. Let $\omega_t = \alpha(1+t)^{-1/2}$ with $0 < \alpha < 2/(L\mu_2)$. Then, ω_t violates the condition (5) while it attains

$$\mathbb{E}[C(\theta^{(\tau_T)}, \xi^{(\tau_T)})] = \mathcal{O}(T^{-1/4}(\log T)^{1/2}).$$

Extending the Corollary 1, we can also prove that $\beta = 1/2$ yields the fastest convergence rate (in terms of the upper-bound) among the learning rate schedule $\omega_t = (1+t)^{-\beta}$, $\beta > 0$. As it diverges from the main focus of this paper, it will be omitted.

Table 1: Synthetic dataset experiments. The proposed approach (NN with ARTL) is compared with robust regression methods. The **best score** is bolded and blue-colored, and the second best score is underlined.

	checkered	Non-linear volcano	stripe	Linear plane
Linear Reg. with Huber’s Loss	0.124 (0.004)	0.130 (0.003)	0.498 (0.016)	<u>0.001</u> (0.001)
Linear Reg. with RANSAC	0.140 (0.013)	0.186 (0.058)	0.871 (0.277)	0.001 (0.001)
Support Vector Reg. with RBF Kernel	0.127 (0.008)	0.113 (0.020)	0.508 (0.031)	0.006 (0.002)
NN with Huber’s Loss	0.634 (0.608)	1.031 (0.861)	0.488 (0.475)	0.043 (0.025)
NN with Tukey’s Loss	0.458 (0.655)	0.413 (0.630)	0.304 (0.395)	0.017 (0.009)
NN with Label Noise Reg.	1.155 (1.068)	0.872 (0.659)	0.561 (0.498)	0.756 (0.945)
NN with RANSAC	0.160 (0.036)	0.142 (0.009)	0.527 (0.018)	0.011 (0.016)
NN with ARTL ($h = 0.9n, k = 1$)	<u>0.088</u> (0.090)	<u>0.082</u> (0.076)	<u>0.223</u> (0.238)	0.010 (0.004)
NN with ARTL ($h = 0.9n, k = 2$)	0.061 (0.016)	0.040 (0.029)	0.119 (0.047)	0.007 (0.001)

4 Experiments

The proposed approach is evaluated through synthetic dataset experiments in Section 4.1. We explore parameter selection via cross-validation, utilizing the robust trimmed loss in Section 4.2. Benchmark dataset experiments are conducted in Section 4.3. Source codes to reproduce these experimental results are provided in <https://github.com/oknakfm/ARTL>.

4.1 Synthetic Dataset Experiments

In this section, we assess the performance of our method on synthetic datasets. We compare it against several robust regression baselines to evaluate their effectiveness in handling outliers.

Dataset Generation: We consider four different ground-truth functions $f(x)$ to generate the datasets:

- checkered: $\sin(2x_1) \cos(2x_2)$,
- volcano: $\exp\left(-\left(\{x_1 - \pi\}^2 + \{x_2 - \pi\}^2 - 1\right)^2\right)$,
- stripe: $\sin(2(x_1 + x_2))$,

- plane: $x_1 - x_2$.

Refer to Figure 5 in Supplement C for an illustration of these functions. For each function, we generate a grid of $n = 10^2 = 100$ data points over the domain $[0, 2\pi]^2$. The input variables (x_1, x_2) are uniformly spaced within this domain. The target variable y is computed by adding Gaussian noise to the true function value: $y = f(x) + \epsilon$, where $\epsilon \sim N(0, 0.2^2)$.

Outlier Injection: To simulate outliers, we introduce anomalies into the dataset by replacing the target values of a small subset of data points. Specifically, we randomly select 3% of the data points and assign their target values as $y_i = 5 + \delta_i$, where δ_i is a small random perturbation sampled uniformly from $[-0.1, 0.1]$.

Implementation Details: All experiments are implemented using Python with the NumPy, PyTorch, and scikit-learn libraries. The neural networks consist of three hidden layers with 100 neurons each (i.e., MLP defined in Section 2.1 with $Q = 3, L_1 = L_2 = L_3 = 100$) and use the sigmoid activation function. Training is performed using the Adam optimizer with a learning rate of 0.01 for 5000 iterations. As a learning rate schedule, step decay (with $\gamma = 0.5$ for each 1000 iteration) is employed. Unless otherwise noted, the HOVR regularization term uses $\lambda = 10^{-3}$, $q = 2$, and $w_i = J^{-1} \mathbb{1}(i_1 = i_2 = \dots = i_k)$.

Baselines: We employ the following baselines.

- Linear regression with a robust Huber’s loss (Huber and Ronchetti, 1981).
- Linear regression with RANSAC (Fischler and Bolles, 1981): An iterative method that fits a model to subsets of the data to identify inliers, effectively excluding outliers from the final model.
- Support vector regression (Drucker et al., 1996): A regression method using the ϵ -insensitive loss function and an RBF kernel to capture nonlinear relationships.
- Neural network with robust Huber’s Loss (Huber and Ronchetti, 1981) and Tukey’s biweight loss (Beaton and Tukey, 1974). Tukey’s loss is implemented using the constant $c = 4.685$.
- Neural network with a label noise regularization (Han et al., 2020), that is designed to mitigate the impact of noisy labels.
- Neural Network with RANSAC-like Approach (Choi et al., 2009): A neural network that iteratively excludes high-loss samples during training, similar to the RANSAC method (Fischler and Bolles, 1981).

Our proposed method, SGSD applied to TTL+HOVR, is evaluated with different two orders of derivatives $k \in \{1, 2\}$. h is specified as a rounded integer of $0.9n$.

Evaluation Metrics: We assess the performance of each method using the predictive mean squared error (PMSE) on a separate test set of $n_{\text{test}} = 10^4$ randomly sampled points from the same domain. Each experiment is repeated five times with different random seeds, and we report the mean and standard deviation of the PMSE across these runs.

Results: Experimental results are summarized in Table 1. Visualization of the estimated functions is also listed in Supplement C. Our interpretation is summarized as follows.

For the linear ‘plane’ function, which can be effectively modeled by simple linear approaches, linear regression using robust loss functions achieves excellent prediction accuracy. While simpler models like linear regression and support vector regression are well-suited for predicting linear functions, the proposed approach using neural network at least achieves the best performance among neural network-based methods.

In contrast, for the non-linear ‘checkered’, ‘volcano’, and ‘stripe’ functions, simpler models are unable to capture the complex patterns. The proposed neural network with TTL+HOVR achieves the best scores across all methods. It is important to note that neural networks trained with robust loss functions, such as Huber’s and Tukey’s, tend to overfit to outliers, as illustrated in Figure 1.

Ablation Study: To demonstrate the effectiveness of combining trimmed loss with HOVR, we present an ablation study in Figure 2 with the ‘checkered’ function. As we can easily examine, (b): The NN trained with the trimmed loss (without HOVR) reduces the overall influence of the outliers due to the robust loss but still overfits to the outliers themselves. As a result, the non-outlier regions are correctly estimated, but sharp peaks appear near the outliers. (c): The influence of outliers is not properly handled by the NN trained only with HOVR (without the robust loss). The regularization suppresses the overall variability of the neural network, but the presence of outliers affects not only the regions with outliers but also other areas of the entire covariate space. (d): The proposed ARTL (TTL+HOVR) yields significantly improved results.

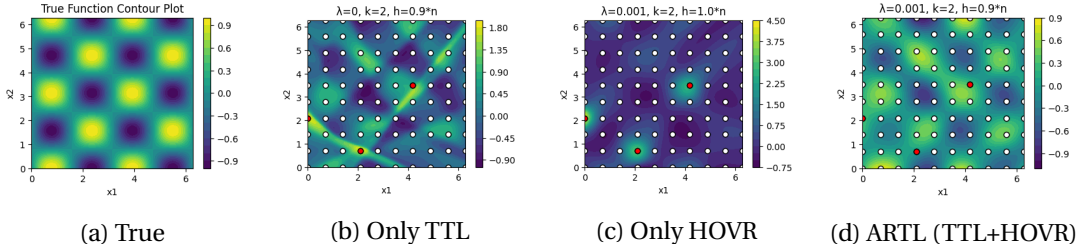


Figure 2: Ablation study.

The average PMSE values (and the standard deviations) are: (b) 0.187 (0.021), (c) 0.356 (0.057), (d) 0.064 (0.005), and these values clearly highlight the superior performance of our proposed approach (ARTL).

Computational Time: We compare the computational time required to train the neural network using ARTL (TTL+HOVR) versus TTL alone. On average, across 10 trials using Tesla T4 processor (15.84GB memories), ARTL takes 19.598 seconds to complete 5000 iterations, while TTL (without HOVR) takes 19.515 seconds. This shows that incorporating HOVR has only a minimal effect on the overall computational time thanks to SGSD not requiring increasing mini-batch size as discussed in Section 2.4. Also see Figure 3 for the progress of the cumulative computational time per iteration.

4.2 Robust Parameter Selection

In this section, we discuss the process of robust parameter selection within our proposed framework. The robust validation score is defined as follows:

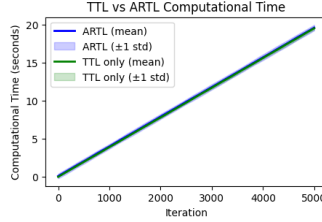


Figure 3: Accumulated computational time.

Table 2: Benchmark dataset experiments. The proposed approach (NN with ARTL) is compared with robustly trained neural networks. The **best score** is bolded and blue-colored, and the second best score is underlined.

	Auto MPG	Liver Disorders	Real Estate Valuation
NN with Huber’s Loss	0.808 (0.363)	3.269 (0.798)	2.148 (0.710)
NN with Tukey’s Loss	1.126 (0.839)	2.976 (0.477)	2.127 (0.746)
NN with Label Noise Reg.	0.751 (0.410)	2.016 (0.319)	1.433 (0.383)
NN with RANSAC	1.078 (0.172)	1.146 (0.158)	1.087 (0.158)
NN with ARTL ($h = 0.9n, k = 1, \lambda = 10^{-4}$)	0.229 (0.040)	1.617 (0.273)	0.470 (0.132)
NN with ARTL ($h = 0.9n, k = 1, \lambda = 10^{-3}$)	0.211 (0.038)	<u>1.546</u> (0.190)	0.453 (0.144)
NN with ARTL ($h = 0.9n, k = 2, \lambda = 10^{-4}$)	0.228 (0.053)	1.554 (0.295)	<u>0.467</u> (0.166)
NN with ARTL ($h = 0.9n, k = 2, \lambda = 10^{-3}$)	<u>0.223</u> (0.064)	1.633 (0.145)	0.479 (0.155)

Robust Validation Score: We start by splitting the outlier-contaminated data into a training set (80%) and a validation set (20%). The validation score is computed using the robust trimmed loss ($h = 0.9n$).

In this experiment, we compute the average PMSE over 10^4 randomly generated test samples (excluding outliers) and the average validation score (using the outlier-contaminated data) across 10 trials, each with a different random seed. The majority of the experimental settings are inherited from Section 4.1.

Results: Figure 4 presents the results. The averaged PMSE and the averaged validation scores are displayed, with error bars indicating the standard deviation. The strong correlation highlights that the robust validation score, based on the trimmed loss, is a reliable estimator of PMSE. Consequently, we think that this robust validation score can be effectively used for parameter selection, even in the presence of outliers.

4.3 Benchmark Dataset Experiments

We validate our proposed algorithm through experiments on typical benchmark datasets: the Auto MPG, Liver Disorders, and Real Estate Valuation datasets from the UCI Machine Learning Repository (Kelly et al., 2023)¹, with artificially introduced outliers. For the Auto MPG dataset, the ‘origin’ and ‘car_name’ columns were removed, and for the Real Estate Valuation dataset, the ‘X1 transaction date’, ‘X5 latitude’, and ‘X6 longitude’ columns were excluded due to a data type issue. Consequently, the sample size and the covariate dimensions are, $n = 398, J = 5$ for Auto MPG,

¹<https://archive.ics.uci.edu>

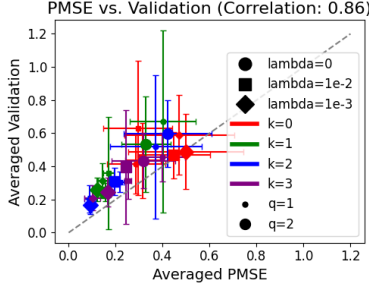


Figure 4: The average robust validation scores are compared with the average PMSE, in the presence of outliers. The Pearson correlation coefficient between the averaged values is 0.86, and the Spearman’s rank correlation coefficient is 0.89.

$n = 345, J = 5$ for Liver Disorders, and $n = 414, J = 3$ for Real Estate Valuation datasets. Implementation details are inherited from Section 4.1.

Dataset Formatting: In each experiment among 5 runs, we randomly split each dataset into a training set (70%) and a test set (30%). To introduce outliers, 5% of the outcomes in the training set are randomly selected and modified by adding two times the standard deviation to their original values.

Baselines: We utilize non-linear neural networks with Huber’s and Tukey’s loss functions, label noise regularization, and RANSAC, as also employed in synthetic dataset experiments in Section 4.1.

Results: Experimental results are summarized in Table 2. Average PMSE among the 5 runs is provided with the standard deviation in the parenthesis. For all datasets, the proposed method consistently achieves the best or nearly best results. While the RANSAC approach yields the top score for the Liver Disorders dataset, its performance is unstable, and it produces the second worst score for the Auto MPG dataset.

5 Conclusion

In this study, we introduced a stochastic algorithm called stochastic gradient-supergradient descent (SGSD) for training neural networks using the augmenter and regularized trimmed loss (ARTL). ARTL combines transformed trimmed loss (TTL) with higher-order variation regularization (HOVR). We provided a theoretical proof of SGSD’s convergence and demonstrated its effectiveness through experiments. A key advantage of our method, in contrast to techniques like splines, is its broad applicability to a wide range of models, including neural networks with complex architectures.

Acknowledgement

A. Okuno was supported by JSPS KAKENHI (21K17718, 22H05106). We would like to thank Hironori Fujisawa and Keisuke Yano for the helpful discussions.

References

- Alfons, A., Croux, C., and Gelper, S. (2013). Sparse least trimmed squares regression for analyzing high-dimensional large data sets. *The Annals of Applied Statistics*, 7(1):226–248.
- Aravkin, A. and Davis, D. (2020). Trimmed statistical estimation via variance reduction. *Mathematics of Operations Research*, 45(1):292–322.
- Bartolucci, F., De Vito, E., Rosasco, L., and Vigogna, S. (2023). Understanding neural networks with reproducing kernel banach spaces. *Applied and Computational Harmonic Analysis*, 62:194–236.
- Beaton, A. E. and Tukey, J. W. (1974). The fitting of power series, meaning polynomials, illustrated on band-spectroscopic data. *Technometrics*, 16(2):147–185.
- Beck, A. (2017). *First-order methods in optimization*. SIAM.
- Bottou, L., Curtis, F. E., and Nocedal, J. (2018). Optimization methods for large-scale machine learning. *SIAM review*, 60(2):223–311.
- Bredies, K. and Holler, M. (2020). Higher-order total variation approaches and generalisations. *Inverse Problems*, 36(12):123001.
- Brown, T., Mann, B., Ryder, N., Subbiah, M., Kaplan, J. D., Dhariwal, P., Neelakantan, A., Shyam, P., Sastry, G., Askell, A., et al. (2020). Language models are few-shot learners. *Advances in Neural Information Processing Systems*, 33:1877–1901.
- Choi, S., Kim, T., and Yu, W. (2009). Performance evaluation of RANSAC family. In *Proceedings of the British Machine Vision Conference*, pages 1–12. British Machine Vision Association.
- Cybenko, G. (1989). Approximation by superpositions of a sigmoidal function. *Mathematics of Control, Signals and Systems*, 2(4):303–314.
- Deleu, T. and Bengio, Y. (2021). Structured sparsity inducing adaptive optimizers for deep learning. *arXiv preprint arXiv:2102.03869*.
- Drucker, H., Burges, C. J., Kaufman, L., Smola, A., and Vapnik, V. (1996). Support vector regression machines. *Advances in Neural Information Processing Systems*, 9.
- Duan, J., Ding, Y., Pan, Z., Yang, J., and Bai, L. (2015). Second order mumford-shah model for image denoising. In *Proceedings of the 2015 IEEE International Conference on Image Processing*, pages 547–551.
- Engl, H. W., Hanke, M., and Neubauer, A. (1996). *Regularization of inverse problems*, volume 375. Springer Science & Business Media.
- Fischler, M. A. and Bolles, R. C. (1981). Random sample consensus: a paradigm for model fitting with applications to image analysis and automated cartography. *Commun. ACM*, 24(6):381–395.
- Ghadimi, S. and Lan, G. (2013). Stochastic first-and zeroth-order methods for nonconvex stochastic programming. *SIAM Journal on Optimization*, 23(4):2341–2368.
- Goodfellow, I., Bengio, Y., and Courville, A. (2016). *Deep Learning*. MIT Press. <http://www.deeplearningbook.org>.

- Han, B., Niu, G., Yu, X., Yao, Q., Xu, M., Tsang, I., and Sugiyama, M. (2020). SIGUA: Forgetting may make learning with noisy labels more robust. In *International Conference on Machine Learning*, pages 4006–4016.
- Hernández-García, A. and König, P. (2018). Data augmentation instead of explicit regularization. *arXiv preprint arXiv:1806.03852*.
- Hinterberger, W. and Scherzer, O. (2006). Variational methods on the space of functions of bounded hessian for convexification and denoising. *Computing*, 76:109–133.
- Huber, P. and Ronchetti, E. (1981). *Robust Statistics*. Wiley Series in Probability and Statistics. Wiley.
- Kelly, M., Longjohn, R., and Nottingham, K. (2023). The UCI Machine Learning Repository.
- Kingma, D. P. and Ba, J. (2014). Adam: A method for stochastic optimization. *arXiv preprint arXiv:1412.6980*.
- Koenker, R. and Mizera, I. (2004). Penalized triograms: total variation regularization for bivariate smoothing. *Journal of the Royal Statistical Society: Series B (Statistical Methodology)*, 66(1):145–163.
- Liu, P., Yuan, W., Fu, J., Jiang, Z., Hayashi, H., and Neubig, G. (2023). Pre-train, prompt, and predict: A systematic survey of prompting methods in natural language processing. *ACM Computing Surveys*, 55(9):1–35.
- Luo, P., Wang, X., Shao, W., and Peng, Z. (2019). Towards understanding regularization in batch normalization. In *International Conference on Learning Representations*.
- Mammen, E. and van de Geer, S. (1997). Locally adaptive regression splines. *The Annals of Statistics*, 25(1):387–413.
- Metel, M. and Takeda, A. (2019). Simple stochastic gradient methods for non-smooth non-convex regularized optimization. In *International Conference on Machine Learning*, pages 4537–4545. PMLR.
- Metel, M. R. and Takeda, A. (2021). Stochastic proximal methods for non-smooth non-convex constrained sparse optimization. *Journal of Machine Learning Research*, 22(115):1–36.
- Miikkulainen, R., Liang, J., Meyerson, E., Rawal, A., Fink, D., Francon, O., Raju, B., Shahrzad, H., Navruzyan, A., Duffy, N., and Hodjat, B. (2019). Chapter 15 - Evolving Deep Neural Networks. In *Artificial Intelligence in the Age of Neural Networks and Brain Computing*, pages 293–312. Academic Press.
- Osher, S., Burger, M., Goldfarb, D., Xu, J., and Yin, W. (2005). An iterative regularization method for total variation-based image restoration. *Multiscale Modeling & Simulation*, 4(2):460–489.
- Parhi, R. and Nowak, R. D. (2021). Banach space representer theorems for neural networks and ridge splines. *Journal of Machine Learning Research*, 22(43):1–40.
- Parhi, R. and Nowak, R. D. (2022). What kinds of functions do deep neural networks learn? insights from variational spline theory. *SIAM Journal on Mathematics of Data Science*, 4(2):464–489.
- Robbins, H. and Monro, S. (1951). A stochastic approximation method. *The Annals of Mathematical Statistics*, 22(3):400–407.

- Rousseeuw, P. J. (1984). Least median of squares regression. *Journal of the American statistical association*, 79(388):871–880.
- Rudin, L. I., Osher, S., and Fatemi, E. (1992). Nonlinear total variation based noise removal algorithms. *Physica D: Nonlinear Phenomena*, 60(1):259–268.
- Samek, W., Montavon, G., Lapuschkin, S., Anders, C. J., and Müller, K.-R. (2021). Explaining deep neural networks and beyond: A review of methods and applications. *Proceedings of the IEEE*, 109(3):247–278.
- Smale, S. and Zhou, D.-X. (2007). Learning theory estimates via integral operators and their approximations. *Constructive Approximation*, 26(2):153–172.
- Srivastava, N., Hinton, G., Krizhevsky, A., Sutskever, I., and Salakhutdinov, R. (2014). Dropout: A simple way to prevent neural networks from overfitting. *Journal of Machine Learning Research*, 15(56):1929–1958.
- Stone, C. J. (1994). The Use of Polynomial Splines and Their Tensor Products in Multivariate Function Estimation. *The Annals of Statistics*, 22(1):118 – 171.
- Sze, V., Chen, Y.-H., Yang, T.-J., and Emer, J. S. (2017). Efficient processing of deep neural networks: A tutorial and survey. *Proceedings of the IEEE*, 105(12):2295–2329.
- Unser, M. (2023). Ridges, neural networks, and the radon transform. *Journal of Machine Learning Research*, 24(37):1–33.
- Williams, F., Trager, M., Bruna, J., and Zorin, D. (2021). Neural Splines: Fitting 3d Surfaces With Infinitely-Wide Neural Networks. In *Proceedings of the IEEE/CVF Conference on Computer Vision and Pattern Recognition*, pages 9949–9958.
- Xu, Y., Jin, R., and Yang, T. (2019a). Non-asymptotic analysis of stochastic methods for non-smooth non-convex regularized problems. *Advances in Neural Information Processing Systems*, 32.
- Xu, Y., Qi, Q., Lin, Q., Jin, R., and Yang, T. (2019b). Stochastic optimization for DC functions and non-smooth non-convex regularizers with non-asymptotic convergence. In *Proceedings of the 36th International Conference on Machine Learning*, volume 97, pages 6942–6951. PMLR.
- Yagishita, S. (2024). Fast algorithm for sparse least trimmed squares via trimmed-regularized reformulation. *arXiv preprint arXiv:2410.04554*.
- Yao, Y., Rosasco, L., and Caponnetto, A. (2007). On early stopping in gradient descent learning. *Constructive Approximation*, 26:289–315.
- Yarotsky, D. (2017). Error bounds for approximations with deep ReLU networks. *Neural Networks*, 94:103–114.
- Yun, J., Lozano, A. C., and Yang, E. (2021). Adaptive proximal gradient methods for structured neural networks. *Advances in Neural Information Processing Systems*, 34:24365–24378.
- Zhang, C., Bengio, S., Hardt, M., Recht, B., and Vinyals, O. (2021). Understanding deep learning (still) requires rethinking generalization. *Communication of the ACM*, 64(3):107–115.
- Zou, H. and Hastie, T. (2005). Regularization and variable selection via the elastic net. *Journal of the Royal Statistical Society Series B: Statistical Methodology*, 67(2):301–320.

Supplementary Materials

- (Title) Outlier-Robust Neural Network Training: Efficient Optimization of Transformed Trimmed Loss with Variation Regularization
- (Authors) Akifumi Okuno and Shotaro Yagishita

A Regularization for Simpler Models

A linear basis function model $f_\theta^\dagger(x) = \sum_{l=1}^L \theta_l \phi_l(x)$ with user-specified basis functions $\{\phi_l\}$ encompasses kernel and spline regression models as special cases. Here, consider the univariate case $J = 1$ for simplicity. With the gram matrix $G^{[k]} = (g_{ij}^{[k]})$, $g_{ij}^{[k]} = \int_{\Omega} \nabla^{[k]} \phi_i(x) \nabla^{[k]} \phi_j(x) dx$, we have

$$\begin{aligned} \|\nabla^{[k]} f_\theta^\dagger\|_{L^2(\Omega)}^2 &= \int_{\Omega} \|\nabla^{[k]} f_\theta^\dagger(x)\|^2 dx \\ &= \sum_{l_1=1}^L \sum_{l_2=1}^L \theta_{l_1} \theta_{l_2} \underbrace{\int_{\Omega} \nabla^{[k]} \phi_{l_1}(x) \nabla^{[k]} \phi_{l_2}(x) dx}_{=g_{l_1 l_2}^{[k]}} \\ &= \sum_{l_1=1}^L \sum_{l_2=1}^L \theta_{l_1} \theta_{l_2} g_{l_1 l_2}^{[k]} = \langle \theta, G^{[k]} \theta \rangle. \end{aligned}$$

It also reduces to the ridge regularization $\|\theta\|_2^2$ by assuming that $\{\nabla^{[k]} \phi_l\}$ is orthonormal (i.e., $G^{[k]}$ is an identity matrix). See, e.g., [Smale and Zhou \(2007\)](#) for more details of the regularization for kernel regression.

B Detailed Proofs

B.1 Derivation of Assumption 1(c)

As it holds that

$$\mathbb{E}[\langle \Delta u_{h,\lambda}^{(t)}, g_{h,\lambda}(\theta^{(t)}, \xi^{(t)}) \rangle] = \mathbb{E}[\mathbb{E}_t[\langle \Delta u_{h,\lambda}^{(t)}, g_{h,\lambda}(\theta^{(t)}, \xi^{(t)}) \rangle]] = \mathbb{E}[\underbrace{\langle \mathbb{E}_t[\Delta u_{h,\lambda}^{(t)}], g_{h,\lambda}(\theta^{(t)}, \xi^{(t)}) \rangle}_{=0}] = 0, \quad (6)$$

we have

$$\begin{aligned} \mathbb{E}[\|g_{h,\lambda}^{(t)}(\theta^{(t)}, \xi^{(t)})\|_2^2] &= \mathbb{E}[\|\Delta u_{h,\lambda}^{(t)} + g_{h,\lambda}(\theta^{(t)}, \xi^{(t)})\|_2^2] \\ &= \mathbb{E}[\|\Delta u_{h,\lambda}^{(t)}\|_2^2] + 2 \underbrace{\mathbb{E}[\langle \Delta u_{h,\lambda}^{(t)}, g_{h,\lambda}(\theta^{(t)}, \xi^{(t)}) \rangle]}_{=0 \text{ (equation (6))}} + \mathbb{E}[\|g_{h,\lambda}(\theta^{(t)}, \xi^{(t)})\|_2^2] \\ &\leq \sigma^2 + \mathbb{E}[\|g_{h,\lambda}(\theta^{(t)}, \xi^{(t)})\|_2^2]. \end{aligned}$$

B.2 Proof of Theorem 1

To prove Theorem 1, we present the following lemma.

Lemma 2. Suppose that Assumption 1 holds. Then, it holds that

$$\sum_{t=0}^T (2\omega_t - L\mu_2 \omega_t^2) \mathbb{E}[C(\theta^{(t)}, \xi^{(t)})^2] \leq 2F_{h,\lambda}(\theta^{(0)}, \xi^{(0)}) + L\mu_1 \sum_{t=0}^T \omega_t^2 \quad (7)$$

for any $T \geq 0$.

Proof. As the inequality

$$\begin{aligned} C(\theta^{(t)}, \xi^{(t)}) &= \inf_{v \in \partial V_h(\xi^{(t)})} \|\partial U_\lambda(\theta^{(t)}, \xi^{(t)}) / \partial(\theta, \xi) - (0, v)\|_2 \\ &\leq \|\partial U_\lambda(\theta^{(t)}, \xi^{(t)}) / \partial(\theta, \xi) - (0, v_h(\xi^{(t)}))\|_2 \\ &= \|g_{h,\lambda}(\theta^{(t)}, \xi^{(t)})\|_2 \end{aligned}$$

holds, it suffices to prove that $\sum_{t=0}^T (2\omega_t - L\mu_2\omega_t^2) \mathbb{E}[\|g_{h,\lambda}(\theta^{(t)}, \xi^{(t)})\|_2^2]$ (which upper-bounds the left-hand side of (7)) is upper-bounded by the right-hand side of (7).

Since $\partial U_\lambda / \partial(\theta, \xi)$ is Lipschitz continuous with the Lipschitz constant L , it follows from the well-known descent lemma (Beck, 2017, Lemma 5.7) that

$$\begin{aligned} &U_\lambda(\theta^{(t+1)}, \xi^{(t+1)}) \\ &\leq U_\lambda(\theta^{(t)}, \xi^{(t)}) + \langle \partial U_\lambda(\theta^{(t)}, \xi^{(t)}) / \partial(\theta, \xi), (\theta^{(t+1)}, \xi^{(t+1)}) - (\theta^{(t)}, \xi^{(t)}) \rangle + \frac{L}{2} \|(\theta^{(t+1)}, \xi^{(t+1)}) - (\theta^{(t)}, \xi^{(t)})\|_2^2. \end{aligned}$$

On the other hand, the definition of the subgradient v_h implies that

$$-V_h(\xi^{(t+1)}) \leq -V_h(\xi^{(t)}) - \langle v_h(\xi^{(t)}), \xi^{(t+1)} - \xi^{(t)} \rangle.$$

Consequently, we have

$$\begin{aligned} &F_{h,\lambda}(\theta^{(t+1)}, \xi^{(t+1)}) \\ &\leq F_{h,\lambda}(\theta^{(t)}, \xi^{(t)}) + \langle g_{h,\lambda}(\theta^{(t)}, \xi^{(t)}), (\theta^{(t+1)}, \xi^{(t+1)}) - (\theta^{(t)}, \xi^{(t)}) \rangle + \frac{L}{2} \|(\theta^{(t+1)}, \xi^{(t+1)}) - (\theta^{(t)}, \xi^{(t)})\|_2^2 \\ &= F_{h,\lambda}(\theta^{(t)}, \xi^{(t)}) - \omega_t \langle g_{h,\lambda}(\theta^{(t)}, \xi^{(t)}), g_{h,\lambda}^{(t)}(\theta^{(t)}, \xi^{(t)}) \rangle + \frac{L\omega_t^2}{2} \|g_{h,\lambda}^{(t)}(\theta^{(t)}, \xi^{(t)})\|_2^2. \end{aligned}$$

Taking the expectation yields

$$\begin{aligned} &\mathbb{E}[F_{h,\lambda}(\theta^{(t+1)}, \xi^{(t+1)})] \\ &\leq \mathbb{E}[F_{h,\lambda}(\theta^{(t)}, \xi^{(t)})] - \omega_t \mathbb{E}[\langle g_{h,\lambda}(\theta^{(t)}, \xi^{(t)}), g_{h,\lambda}^{(t)}(\theta^{(t)}, \xi^{(t)}) \rangle] + \frac{L\omega_t^2}{2} \mathbb{E}[\|g_{h,\lambda}^{(t)}(\theta^{(t)}, \xi^{(t)})\|_2^2] \\ &\stackrel{\text{Tower property}}{=} \mathbb{E}[F_{h,\lambda}(\theta^{(t)}, \xi^{(t)})] - \omega_t \mathbb{E}[\mathbb{E}_t[\langle g_{h,\lambda}(\theta^{(t)}, \xi^{(t)}), g_{h,\lambda}^{(t)}(\theta^{(t)}, \xi^{(t)}) \rangle]] + \frac{L\omega_t^2}{2} \mathbb{E}[\|g_{h,\lambda}^{(t)}(\theta^{(t)}, \xi^{(t)})\|_2^2] \\ &= \mathbb{E}[F_{h,\lambda}(\theta^{(t)}, \xi^{(t)})] - \omega_t \mathbb{E}[\langle \mathbb{E}_t[g_{h,\lambda}(\theta^{(t)}, \xi^{(t)})], g_{h,\lambda}^{(t)}(\theta^{(t)}, \xi^{(t)}) \rangle] + \frac{L\omega_t^2}{2} \mathbb{E}[\|g_{h,\lambda}^{(t)}(\theta^{(t)}, \xi^{(t)})\|_2^2] \\ &\stackrel{\text{Assumption 1(b)}}{=} \mathbb{E}[F_{h,\lambda}(\theta^{(t)}, \xi^{(t)})] - \omega_t \mathbb{E}[\|g_{h,\lambda}(\theta^{(t)}, \xi^{(t)})\|_2^2] + \frac{L\omega_t^2}{2} \mathbb{E}[\|g_{h,\lambda}^{(t)}(\theta^{(t)}, \xi^{(t)})\|_2^2] \\ &\stackrel{\text{Assumption 1(c)}}{\leq} \mathbb{E}[F_{h,\lambda}(\theta^{(t)}, \xi^{(t)})] - \left(\omega_t - \frac{L\mu_2\omega_t^2}{2} \right) \mathbb{E}[\|g_{h,\lambda}(\theta^{(t)}, \xi^{(t)})\|_2^2] + \frac{L\mu_1\omega_t^2}{2}. \end{aligned}$$

By summing up, we obtain

$$\begin{aligned} &\sum_{t=0}^T \left(\omega_t - \frac{L\mu_2\omega_t^2}{2} \right) \mathbb{E}[\|g_{h,\lambda}(\theta^{(t)}, \xi^{(t)})\|_2^2] \leq F_{h,\lambda}(\theta^{(0)}, \xi^{(0)}) - \underbrace{\mathbb{E}[F_{h,\lambda}(\theta^{(T+1)}, \xi^{(T+1)})]}_{\leq 0 \quad (\because F_{h,\lambda} \geq 0)} + \frac{L\mu_1}{2} \sum_{t=0}^T \omega_t^2 \\ &\leq F_{h,\lambda}(\theta^{(0)}, \xi^{(0)}) + \frac{L\mu_1}{2} \sum_{t=0}^T \omega_t^2. \end{aligned}$$

The assertion is proved. \square

Proof of Theorem 1. Lemma 2 yields

$$\begin{aligned}
\mathbb{E} [C(\theta^{(\tau_T)}, \xi^{(\tau_T)})^2] &= \sum_{s=0}^T \mathbb{E} [C(\theta^{(\tau_T)}, \xi^{(\tau_T)})^2 \mid \tau_T = s] \mathbb{P}(\tau_T = s) \\
&= \sum_{s=0}^T \mathbb{E} [C(\theta^{(s)}, \xi^{(s)})^2] \frac{2\omega_s - L\mu_2\omega_s^2}{\sum_{t=0}^T (2\omega_t - L\mu_2\omega_t^2)} \\
&= \underbrace{\left\{ \sum_{s=0}^T (2\omega_s - L\mu_2\omega_s^2) \mathbb{E} [C(\theta^{(s)}, \xi^{(s)})^2] \right\}}_{\leq 2F_{h,\lambda}(\theta^{(0)}, \xi^{(0)}) + L\mu_1 \sum_{t=0}^T \omega_t^2 \quad (\cdot \text{ Lemma 2})} \frac{1}{\sum_{t=0}^T (2\omega_t - L\mu_2\omega_t^2)} \\
&\leq \frac{2F_{h,\lambda}(\theta^{(0)}, \xi^{(0)}) + L\mu_1 \sum_{t=0}^T \omega_t^2}{\sum_{t=0}^T (2\omega_t - L\mu_2\omega_t^2)}. \tag{8}
\end{aligned}$$

Thus, we prove the assertion

$$\mathbb{E} [C(\theta^{(\tau_T)}, \xi^{(\tau_T)})] \stackrel{\text{Cauchy-Schwarz}}{\leq} \mathbb{E} [C(\theta^{(\tau_T)}, \xi^{(\tau_T)})^2]^{1/2} \stackrel{\text{Inequality (8)}}{\leq} \left\{ \frac{2F_{h,\lambda}(\theta^{(0)}, \xi^{(0)}) + L\mu_1 \sum_{t=0}^T \omega_t^2}{\sum_{t=0}^T (2\omega_t - L\mu_2\omega_t^2)} \right\}^{1/2}.$$

□

B.3 Proof of Corollary 1

Proof. As a simple formula indicates

$$\begin{aligned}
\sum_{t=0}^T (1+t)^{-1} &\leq 1 + \int_0^T (1+t)^{-1} dt = 1 + \log(T+1), \text{ and} \\
\sum_{t=0}^T (1+t)^{-1/2} &\geq \int_0^{T+1} (1+t)^{-1/2} dt = 2(T+2)^{1/2} - 2,
\end{aligned}$$

Theorem 1 yields the assertion

$$\begin{aligned}
\mathbb{E} [C(\theta^{(\tau_T)}, \xi^{(\tau_T)})] &\leq \sqrt{\frac{2F_{h,\lambda}(\theta^{(0)}, \xi^{(0)}) + L\mu_1 \alpha^2 \sum_{t=0}^T (1+t)^{-1}}{2\alpha \sum_{t=0}^T (1+t)^{-1/2} - L\mu_2 \alpha^2 \sum_{t=0}^T (1+t)^{-1}}} \\
&\leq \sqrt{\frac{2F_{h,\lambda}(\theta^{(0)}, \xi^{(0)}) + L\mu_1 \alpha^2 + L\mu_1 \alpha^2 \log(T+1)}{4\alpha(T+2)^{1/2} - L\mu_2 \alpha^2 \log(T+1) - 4\alpha - L\mu_2 \alpha^2}} \\
&= \mathcal{O}(T^{-1/4} (\log T)^{1/2}).
\end{aligned}$$

□

C Additional Visualizations

This section provides additional visualizations for the synthetic dataset experiments described in Section 4.1. The four true functions utilized in this study are as follows:

- (checkered) $f_1(x) = \sin(2x_1) \cos(2x_2)$
- (volcano) $f_2(x) = \exp\left(-(\{x_1 - \pi\}^2 + \{x_2 - \pi\}^2 - 1)^2\right)$

- (stripe) $f_3(x) = \sin(2(x_1 + x_2))$
- (plane) $f_4(x) = x_1 - x_2$.

These functions, visualized in Figure 5, serve as the ground truth. The corresponding regression models estimated from outlier-contaminated datasets derived from these functions are presented in Figures 6–9.

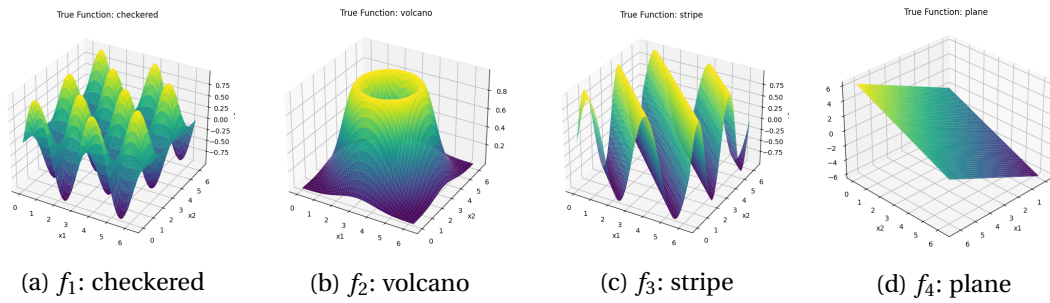


Figure 5: Underlying true functions in our synthetic dataset experiments.

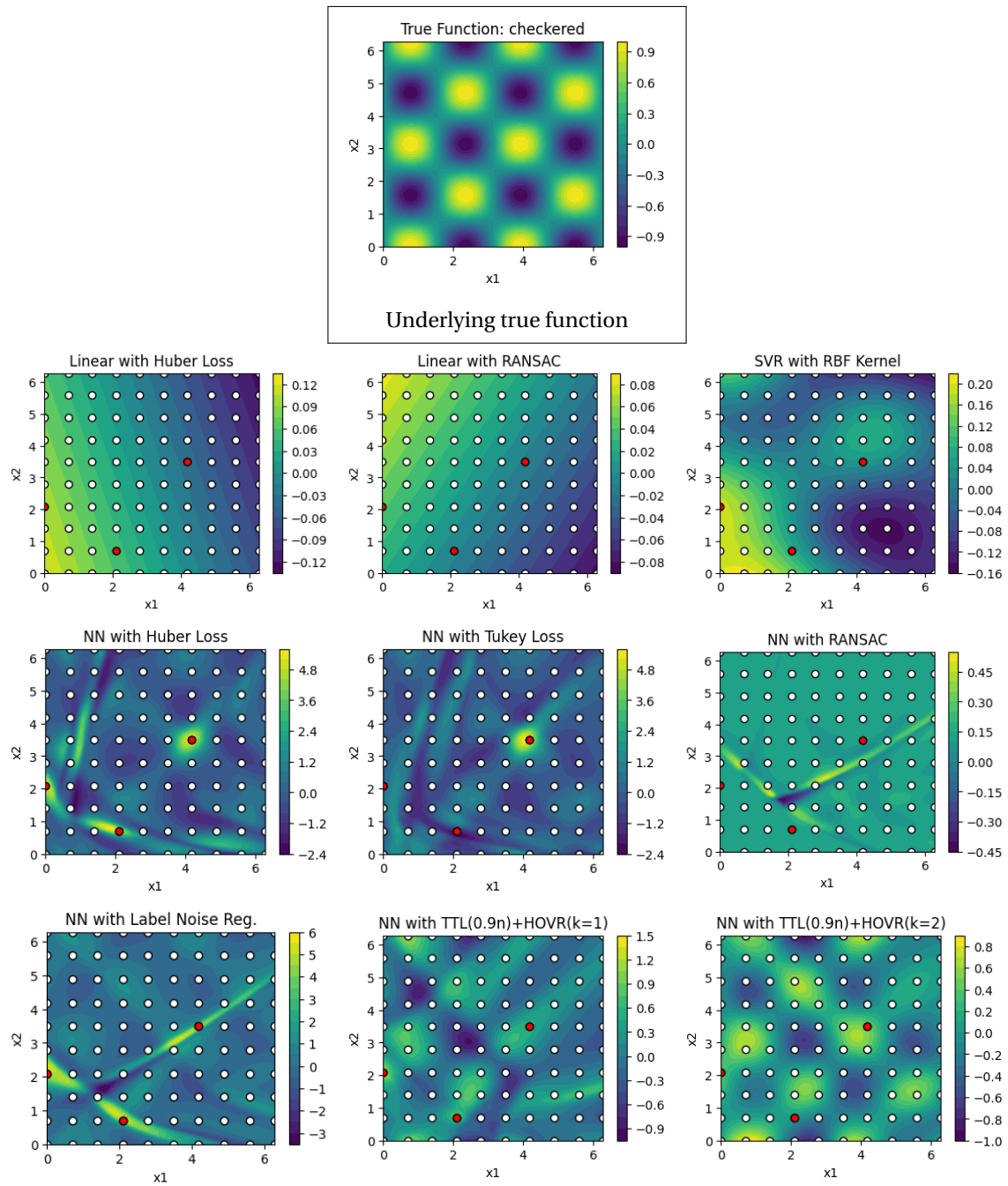


Figure 6: Checkered function $f_1(x) = \sin(2x_1) \cos(2x_2)$.

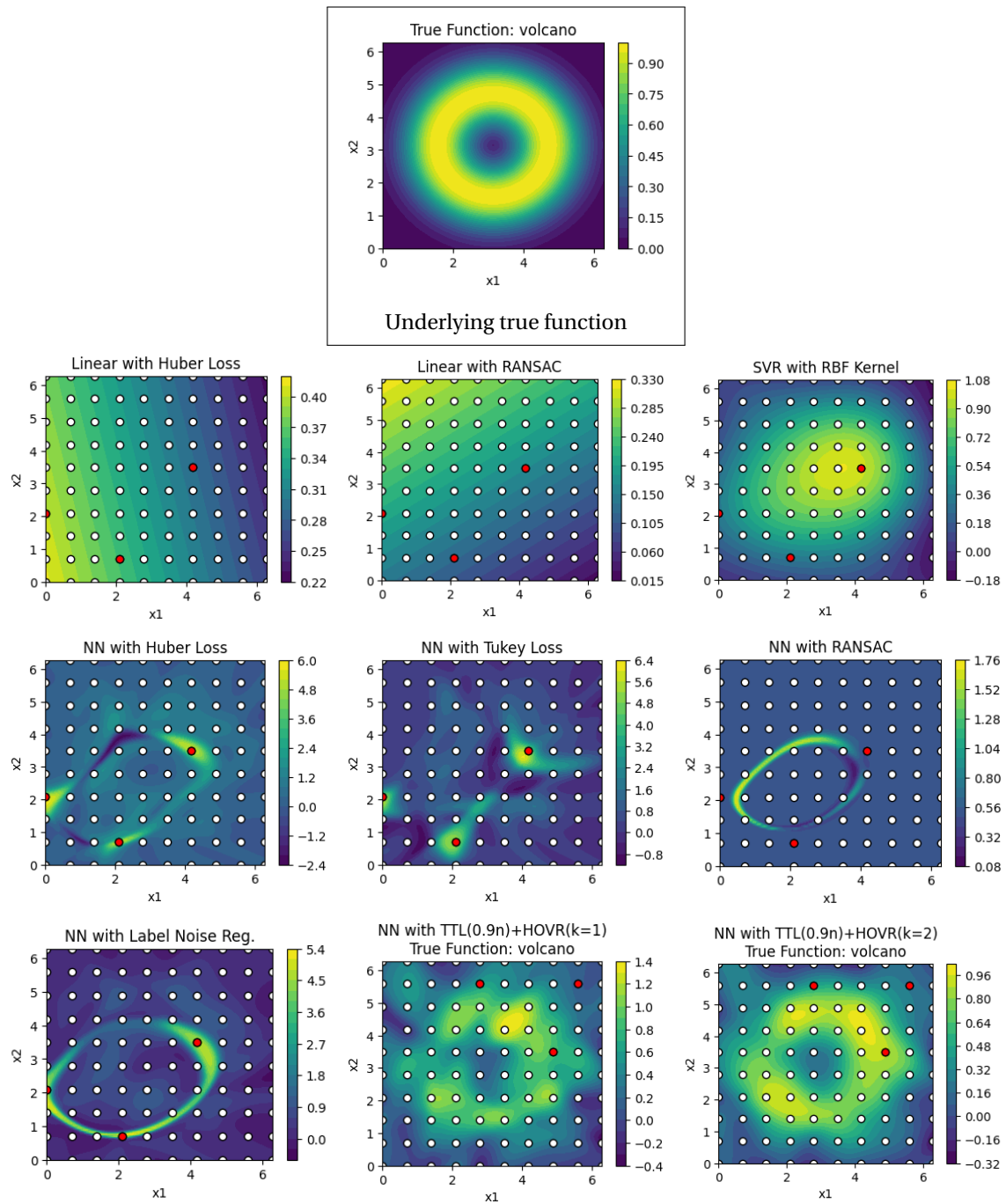


Figure 7: Volcano function $f_2(x) = \exp(-(\{x_1 - \pi\}^2 + \{x_2 - \pi\}^2 - 1)^2)$.

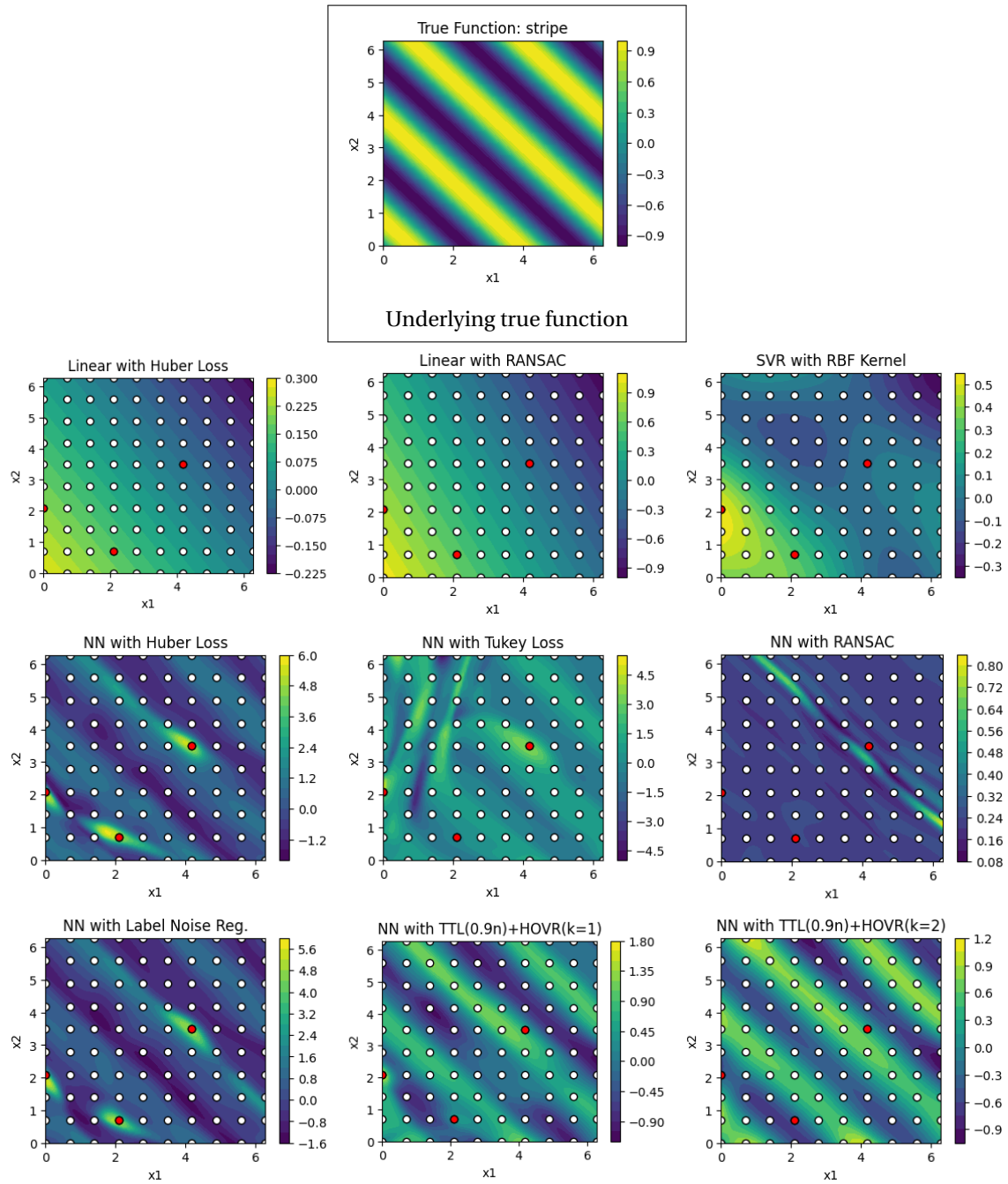


Figure 8: Stripe function $f_3(x) = \sin(2(x_1 + x_2))$.

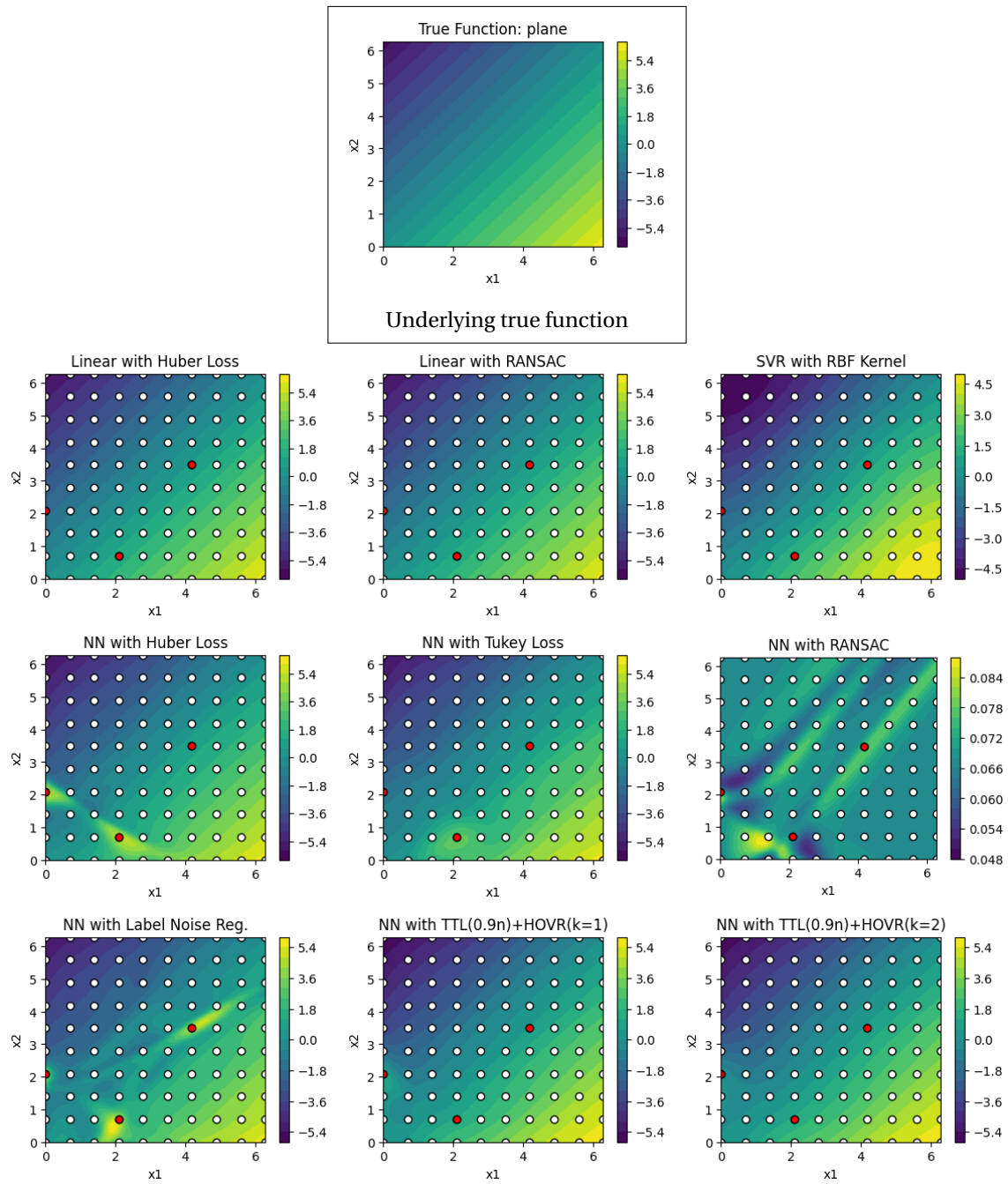


Figure 9: Plane function $f_4(x) = x_1 - x_2$.